Hexagonal Mesophases between Lamellae and Cylinders in a Diblock Copolymer Melt

Ian W. Hamley,*,† Kurt A. Koppi, Jeffrey H. Rosedale, and Frank S. Bates*

Department of Chemical Engineering and Materials Science, University of Minnesota, Minneapolis, Minnesota 55455

Kristoffer Almdal and Kell Mortensen

Risø National Laboratory, DK-4000 Roskilde, Denmark

Received March 29, 1993; Revised Manuscript Received July 26, 1993•

ABSTRACT: Two intermediate phases have been observed upon heating an asymmetric poly(ethylenepropylene)–poly(ethylethylene) diblock copolymer between lamellar and hexagonal cylinder phases near the order–disorder transition. Phase transitions between ordered morphologies are indicated by the temperature dependence of the dynamic shear moduli, and small angle neutron scattering experiments are used to identify these structures as hexagonally modulated lamellae and layered hexagonal packed channels. The observed wavevectors associated with the interlayer scattering for these structures are incommensurate, leading to an aperiodic structure in which the long range translational order of the layers is destroyed. However, the scattering data show that long range in-plane bond orientational order is present, suggesting an analogy with hexatic B phase in liquid crystals. A Fourier imaging method is used to construct density images for the two structures. This shows modulated lamellae for the low temperature phase while channels are evident in the high temperature phase. A restacking transition occurs on shearing the modulated lamellar phase, but the channel phase cannot support large strain shear deformations and instead transforms into rods. These phases do not occur in the mean-field phase diagram for block copolymers, and we believe they are stabilized by composition fluctuations that are the inevitable result of a finite molecular weight. Furthermore, these fluctuations are anisotropic, a feature which has not been accounted for theoretically.

1. Introduction

Block copolymers are proving to be a fascinating class of mesomorphic systems. Although diblock copolymer melts are single component systems in the thermodynamic sense, recent experiments demonstrate that near the order–disorder transition (ODT) they show an unexpectedly rich phase behavior.[1,2] In the vicinity of the ODT, the composition profile (i.e. distribution of, say, the A block) is nearly sinusoidal and mean-field theory accounts for stable lamellar, cylinder, and body-centered cubic phases.[3] This phase diagram is parameterized in terms of the volume fraction of the A block, f, and χN, where χ is the Flory–Huggins segmental interaction parameter and N is the degree of polymerization.

Recent experiments have demonstrated that phases other than the classical ones accounted for in the mean-field theory of Leibler exist near the ODT in diblock copolymer melts.[1,2] The purpose of this paper is to describe detailed experiments on one particular system for which there is a sequence of phases within which we can understand the nature of the transition between lamellae and rods. This is part of a systematic investigation of the phase behavior of diblock copolymers near the ODT.[4] We have studied a poly(ethylenepropylene) (PEP)–poly(ethylethylene) (PEE) diblock copolymer with volume fraction $f = 0.65$ of PEP using dynamic shear modulus measurements and small angle neutron scattering (SANS) experiments of samples dynamically sheared *in situ*. In an earlier report[1] this system was shown to be characterized by multiple ordered phases, although the nonclassical microstructures were not established. Here we show that four phases can be accessed by varying the temperature. These structures are lamellae, hexagonally modulated lamellae, hexagonally packed layered channels, and hexagonally packed cylinders. A more complete compilation of our results on several polyolefin diblock copolymers with $f \simeq 0.65$ will appear elsewhere.[4]

Some of us[5] have recently applied to block copolymers a Landau mean-field theory (due to Marques and Cates,[6] and similar to the approach of Olvera de la Cruz *et al.*[7]) that accounts for certain nonclassical phases near the ordering transition. In this general approach harmonics in the composition profile are allowed for and face-centered cubic (fcc) and square phases can become stable. However, it was shown that for block copolymers the classical phase diagram of Leibler[3] is not modified near the ODT when harmonic corrections are made. Therefore the intermediate hexagonal phases to be described here were not accounted for in this theory. We believe instead that these phases may be stabilized by fluctuations in the composition profile, as we discuss later.

This paper is organized as follows. We first give details of the sample used and experimental methods for the viscoelastic and SANS measurements. Then we present results from dynamic shear modulus measurements which we use to locate phase transitions. SANS experiments used to identify structures are then discussed in detail, along with a Fourier synthesis method of modeling density images. Finally, we summarize our results and discuss them in terms of the phase behavior of mesomorphic systems in general.

2. Experimental Section

Experiments were conducted with a poly(ethylenepropylene)–poly(ethylethylene) (PEP–PEE) diblock copolymer of molecular weight $M_w = 9.4 \times 10^4$ (determined from light scattering experiments) containing 65% PEP by volume. The sample was prepared from anionically polymerized *cis*-1,4-polyisoprene–1,2,-polybutadiene by saturation with deuterium. The deuteration did not lead

* Authors for correspondence.
† Currently at Department of Physics, University of Durham, Science Laboratories, South Road, Durham DH1 3LE, U.K.
• Abstract published in *Advance ACS Abstracts*, October 1, 1993.

0024-9297/93/2226-5959$04.00/0

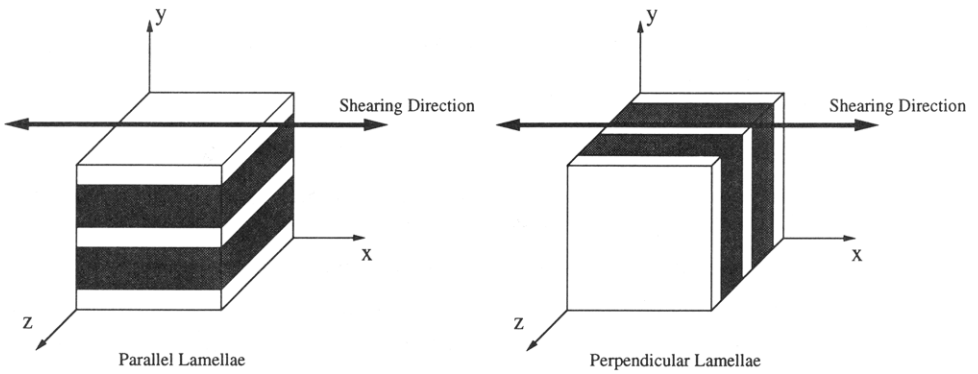

Figure 1. Shearing geometry for SANS experiments. Left, the lamellae are parallel to the shear plane containing the shear direction (x); this is termed the parallel orientation. The neutron beam is incident along y. Right, the lamellae are again parallel to the shear direction, but prependicular to the shear plane. We term this the perpendicular orientation.

to the stoichiometric addition of two deuterons to each double bond. From experiments on homopolymers of similar molecular weight it was found instead that four or five deuterons are associated with each PEP repeat unit, with only about two attached to a PEE unit. This selective deuteration was utilized to provide contrast between the blocks for neutron scattering experiments. The polydispersity, determined by size exclusion chromatography, was $M_w/M_n = 1.05$. Further details of the synthesis are given elsewhere.[8] A sensitive indicator of polymer degradation is the order–disorder transition temperature. This was monitored throughout the series of experiments described here and was found not to vary.

A Rheometrics RSAII rheometer operated with a shear sandwich fixture was used for viscoelastic experiments. These measurements were used to locate phase transitions, by following the temperature dependence of the dynamic elastic shear modulus, G', and the dynamic loss shear modulus, G''. A frequency of $\omega = 0.1$ rad/s was used. This frequency is well below that corresponding to the single copolymer chain relaxation time.[9] The strain amplitude applied was 2%. Numerous isothermal frequency scans were performed, although these are not reported here.

For the small angle neutron scattering (SANS) studies monodomain samples of the copolymer were studied during and after shear, applied using a specially constructed oscillatory shear machine, operating with a simple shear geometry. This device is similar to the one designed by Hadziioannou *et al.*[10] and consists of two parallel aluminum plates ($^1/_{16}$ in. thick) which are recessed into temperature controlled brass heating blocks. A hole was drilled through each block for the unobstructed transmittance of the neutron beam. One block is held stationary and the other is mounted on a motorized screw-driven slider which can be operated between 0.0019 and 4.2 mm/s. Linear oscillatory motion with a minimum displacement of 1.0 mm is achieved using two limit reversing circuits mounted on the slider. Sample thickness can be varied by adjusting the position of the stationary block. The entire shear machine is mounted inside a sealed chamber which can be evacuated and back-filled with helium to minimize any possible sample degradation. The neutron beam is incident through two $^1/_{32}$ in. thick aluminum windows. Apart from preparing well-aligned samples, this device can be used to study the effects of shear on microdomain orientation. In particular it is possible to access two orthogonal orientations from lamellae (see Figure 1.) by varying the temperatures and shear rate, as described elsewhere.[9] Experiments reported here were conducted with 1 mm thick specimens that were subjected to a 100% strain amplitude at frequencies of $0.01 < \omega/\text{rads}^{-1} < 0.2$. The corresponding absolute shear rates are obtained using $|\dot{\gamma}| = 2\gamma\omega/\pi$, where γ is the dimensionless strain.

The SANS experiments were conducted on the NIST/Exxon/University of Minnesota 30-m instrument at the National Institute of Standards and Technology (NIST), Gaithersburg, MD and at the 12-m SANS facility at Risø National Laboratory, Roskilde, Denmark. At NIST, we used $\lambda = 6$ Å neutrons and the wavelength distribution was $\Delta\lambda/\lambda = 0.14$. At Risø we used $\lambda = 5.5$ Å neutrons and the wavelength distribution was $\Delta\lambda/\lambda = 0.09$. Neutron scattering data were collected on an area detector and are reported in arbitrary units of intensity.

3. Rheology Results

Interpretation of the viscoelastic measurements is complicated by many factors, including lack of information on the state of orientation of the sample and the heating/cooling rate dependence of the shear moduli.[11] In addition, the material used in a previous study[1] contained a different degree of isotopic labeling due to variations in the saturation reaction conditions. Varying the level of isotope substitution can change transition temperatures, and also the sequence of phases, for samples derived from the same batch of parent polydiene diblock copolymer.[12] We defer a full discussion of the dependence of the phase diagram of polyolefin diblock copolymers with $f = 0.6$–0.7 on f, N, and isotopic substitution to a future paper.[4] However, we note here that the identical sequence of phases for the PEP–PEE sample discussed in this paper was also found for a poly(ethylene)–poly(ethylethylene) (PE–PEE) diblock with $f_{PE} = 0.65$, $M_w = 4.3 \times 10^4$, and different levels of isotopic substitution (phase transition temperatures were shifted upward by about 2 °C in a sample containing no deuterium compared to one made by hydrogenating a deuterated precursor). The following results are to be viewed as giving evidence for three order–order phase transitions in the system, the exact locations of transition temperatures would require more detailed studies allowing for kinetic effects.

With this caveat, the dynamic shear moduli as a function of temperature on heating at 0.2 °C/min are shown in Figure 2a. Phase transitions beginning at 87 ± 2, 136 ± 2, and 147 ± 2 °C are evident from the sharp changes in both loss and elastic components at these temperatures. The sharpness of the increase in G' at 136 °C depends on the finite heating rate in the experiment (the third ordered phase grows in slowly). However, this study is not concerned with the dynamics of phase transitions, but focuses on the structure of the four ordered phases revealed by rheology. To this end, we took care to measure SANS patterns on developed phases (at 140 °C in the case of the

third phase). It has been shown elsewhere that the first phase transition in this system is reversible, with a hysteresis ~7 °C for a heating and cooling rate of 0.53 °C/min. The sample disorders at 178 ± 2 °C. Figure 2b illustrates that on cooling at 0.4 °C/min a transition from the highest temperature phase to the next ordered phase occurs at a lower temperature than on heating. The system then gets trapped in the high modulus phase down to the lowest temperature at which measurements were performed (75 °C), at least for the time required to conduct these experiments.

Isothermal frequency sweeps revealed different viscoelastic responses in the four phases. The first and second have similar behavior, which indicates that they are topologically similar. The third phase has a much weaker dependence of the moduli on frequency at low frequencies than that for the two lower temperature phases. In addition the modulus decreases on application of a large amplitude (100% strain) shear field. This also occurs for the high temperature phase, in which after large strain shear the low frequency falloff of the moduli is less steep than for the first phase and also shows almost no recovery.

For the structural analysis that follows we will make use of the shear modulus data to locate order–order phase transition temperatures.

4. Small Angle Neutron Scattering Results

A morphology cannot be assigned to a phase based on rheological measurements alone so we turned to SANS, a method well-suited for probing the microstructures in block copolymer melts (with length scales ~hundreds of angströms).

In the following we will discuss the SANS data using the axis system shown for the parallel orientation, although in reality two different orientations (Figure 1) could be accessed by varying the shearing conditions.[9] The neutron beam is incident along y in a laboratory-fixed frame when studying either parallel or perpendicular orientations. The scattering data in the perpendicular orientation to be presented were all obtained after the sample was disordered, then cooled to the desired temperature, and subjected to large amplitude oscillatory shear prior to recording scattering patterns. We found that previous disordering of the sample results in sharper spots in the scattering pattern for the perpendicular orientation, which we interpret as the elimination of defects that are present in the original (lamellar) structure.

The data in Figure 3 were obtained at least 20 min after the shear was switched off, by which time the structure had achieved a steady state, as indicated by the fact that the scattering pattern no longer changed with time. The scattering pattern at 80 °C with the neutron beam incident along z (Figure 3a) shows meridional Bragg peaks at a wavevector $|\mathbf{q}_y| = q^*$ with higher order reflections at $2q^*$ and $3q^*$ (not shown), indicative of a flat lamellar phase. The wavevector $q = 4\pi (\sin\theta)/\lambda$, where θ is half the angle through which the beam is scattered and λ is the wavelength. The assignment of lamellae for the low temperature phase is confirmed by the featureless scattering pattern that results when the neutron beam is incident along y.

When the temperature is increased to a temperature in the next phase (here 120 °C) and after application of a 100% strain amplitude, low frequency shear field, a dramatic transformation of the scattering patterns to those shown in Figure 3b occurs. The parallel orientation can be accessed by heating from the lamellar phase with high strain, low frequency ($|\dot{\gamma}| = 0.006\ s^{-1}$) shear. However, as

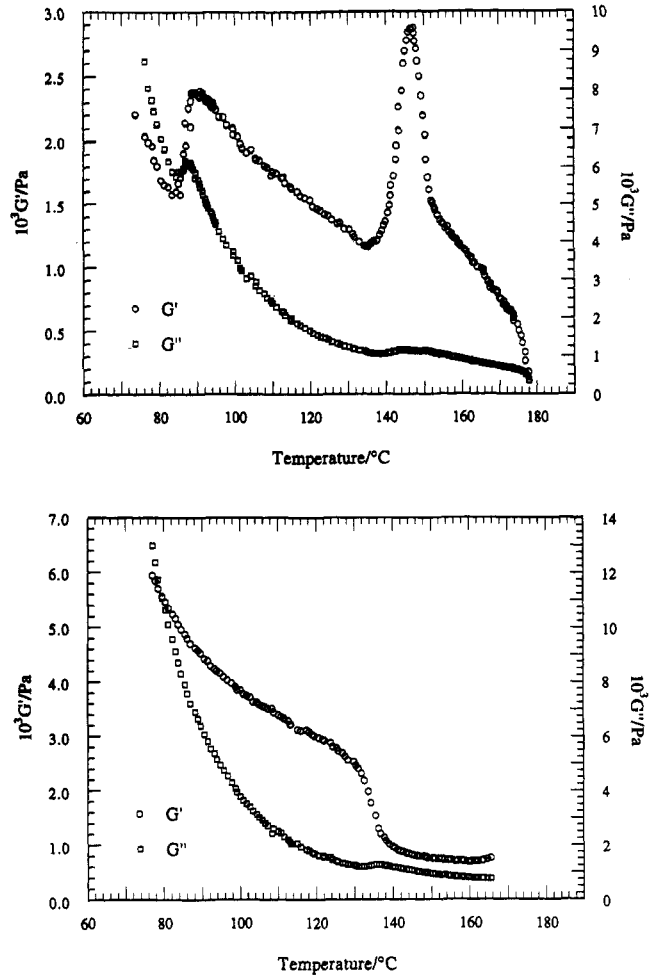

Figure 2. Dynamic storage modulus (circles) and dynamic loss modulus (squares) as a function of temperature, measured at 0.1 rad/s for f = 0.65 PEP–PEE. (a, Top) Heating rate of 0.2 °C/min. Three first order phase transitions are apparent from the changes in the viscoelastic response on heating before the sample disorders at 178 °C. (b, Bottom) Cooling at 0.4 °C/min, beginning from the highest ordered phase at 166 °C. The system appears to get trapped in the channel phase.

mentioned above, a well oriented sample in the perpendicular orientation is obtained under similar shearing conditions but on cooling from the disordered state into the second ordered phase. In the top part of Figure 3b the meridional peaks indicate perpendicularly oriented planes. The four weaker spots are associated with the hexagonal order clearly shown in the scattering pattern with the neutron beam incident along y. These patterns are consistent with a structure such as that sketched in Figure 3b. The lamellae have developed an in-plane hexagonal modulation, with a periodicity 10% larger than the interlayer spacing. Fourier images of this phase will be discussed in the next section. The baroclinic-type mode modulation of the layers in a section (xy) sketched in Figure 3b is only one of a number of possible deformations[13] to be discussed in the next section. An important observation from the scattering data for this phase is that as the block copolymer breaks symmetry from the one-dimensional lamellar phase, two length scales appear, together with a hexagonal modulation.

The reversibility of the lamellae–hexagonally modulated lamellae phase transition was confirmed in SANS experiments in both the parallel and perpendicular orientations. The reversibility of the lamellae–hexagonally modulated lamellae transition was also shown in previous shear modulus measurements.[1] On heating from the lamellar phase to the modulated lamellar phase, the featureless

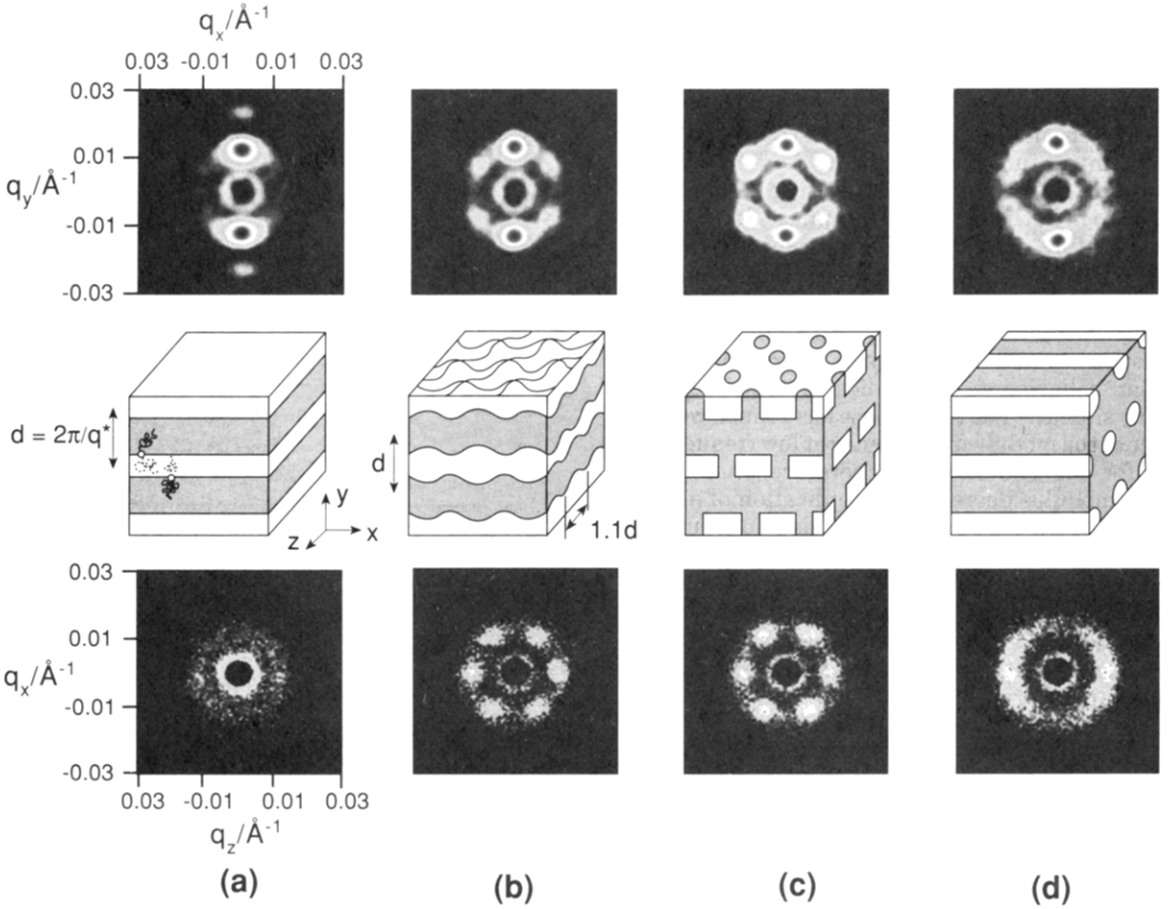

Figure 3. Small angle neutron scattering patterns in two directions, obtained after shearing, together with deduced morphologies for an $f = 0.65$ PEP–PEE diblock at different temperatures. The neutron beam was incident orthogonal to the shear plane. The top series are plotted on a logarithmic scale, while those at the bottom are on a linear scale highlighting changes in scattering intensities in the weak scattering direction. (a) In a low temperature phase the morphology is clearly lamellar. Diblock copolymer chains are shown at the interface. (b) At 120 °C a hexagonally modulated lamellar phase is formed. A break in length scales is shown by the 10% difference in the periodicities in the xz and xy planes. (c) Upon heating into the next phase, hexagonally arranged PEP holes have formed, with the holes sketched here as part of a monocontinuous domain. The holes are drawn as cylinders for simplicity; the exact shape cannot be determined from our data. (d) After heating into the high temperature phase and shearing, rods of the minority component in the PEP matrix are aligned parallel to the shear direction. A possible mechanism for the channel–rod phase transition is illustrated in Figure 8.

scattering pattern in the parallel orientation found at the top of Figure 4a transforms as shown into a pronounced ring of scattering at q^*. On application of a 100% strain amplitude, low frequency shear field (at the same temperature) the pattern shown in the bottom center of Figure 4a evolves, with off-equatorial spots, which have increased in intensity with respect to the unsheared state, as is evident from the angular scans, centered on q^* shown in Figure 5. We interpret this as an enhancement of bond orientational order (i.e. correlation of orientation of the hexagonal nets in different layers; see Figure 6) in the two corresponding hexagonal directions under shear, while it is destroyed along the shear direction. When shearing is stopped, a hexagonal pattern appears. The two equatorial peaks have returned and are in fact 20–30% more intense than the other four. The loss of the two equatorial peaks under shear suggests a restacking transition such as that shown in Figure 7, which indicates a monoclinic-I structure under shear. In the absence of shear we believe that locally the layers are packed in a hexagonal ABAB fashion. On cooling back to the lamellar state, the scattering in the parallel direction again becomes featureless.

In the perpendicular orientation, however, there are no changes in the symmetry of the scattering patterns in the modulated lamellar phase depending on whether the sample is sheared or not (see Figure 4b). However, the four off-axis peaks in the scattering pattern for the sample under shear move to angles larger with respect to the horizontal than those for the unsheared sample, which we interpret in an aperiodic model as being the result of an enhancement of translational order (see next section). The viscoelastic behavior of samples prepared in either an initial parallel or perpendicular lamellar orientation is quite distinct (this anisotropy is discussed in ref 9). Therefore the SANS patterns in two orthogonal directions do not have to be consistent with the same three-dimensional structure. This also supports our subsequent interpretation that these systems possess two-dimensional, rather than crystalline, ordering.

A model for the ordering of the modulations is discussed in the next section in which the incommensurability of the observed wavevectors means that long-range positional order of the modulated lamellae is destroyed. In this case the lattice sites shown in Figure 7 should not be interpreted as implying that there is any long range translational order in the stacking sequence. Instead, it appears that under shear, bond orientational order is destroyed in the shear direction but not in the other hexagonal directions. In the SANS pattern for the sheared sample in the perpendicular orientation (Figure 4b), the side reflections are closer to the closed wavevector circuit condition (60° angle from the vertical) than in the unsheared sample. Within this model, this means that shear has induced more long range translational order, although full three-dimensional

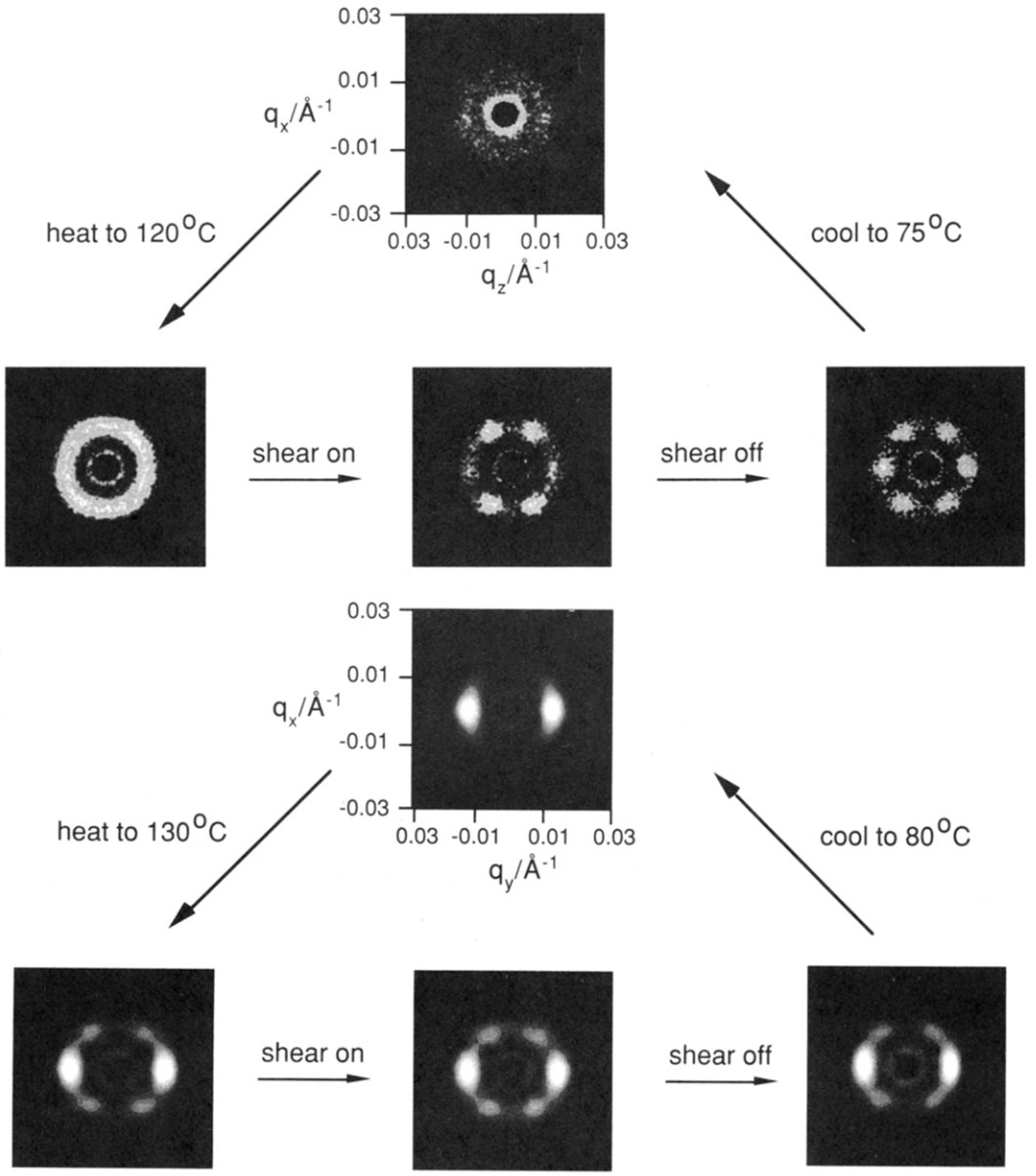

Figure 4. (a, Top) SANS results for the parallel orientation on a linear scale, showing the reversibility of the lamellae–modulated lamellae transition on heating or cooling. In addition, the intermediate scattering pattern observed under shear at $|\dot{\gamma}| = 0.03\ s^{-1}$, 100% strain is shown. In this state, the two first order equatorial reflections are supressed, which we interpret on the basis of a restacking transition (Figure 7). (b, Bottom) In the perpendicular orientation, the symmetry of the SANS patterns (shown on a log scale) is not changed under shear ($|\dot{\gamma}| = 0.1\ s^{-1}$, 100% strain) in the modulated lamellar phase; however the four side peaks now make a larger angle with the horizontal than in the absence of shear (the temperature difference compared to (a) does not affect the symmetry of the scattering patterns).

translational order has still not been established. This is evident because the SANS patterns are not consistent with long range hexagonal ABAB order. An ABAB stacking sequence is likely to be favored locally because it ensures efficient space filling of the modulations, consistent with a two-dimensional baroclinic mode deformation. The fact that the symmetry of these patterns is not changed on shearing supports our interpretation that it is the bond orientation order which is changed on shearing. In an alternative periodic model, the stacking sequence is perturbed from ABAB hexagonal packing due to a successive displacement of layers in a monoclinic structure. Then the sites in Figure 7 are also intended to show the local stacking sequence.

The hexagonal pattern with the beam along y is retained (with little change in intensity) on heating from 120 to 140 °C. In the perpendicular direction, however, the intensities of the four side spots have now increased to about 40% of the intensity of the two principal equatorial reflections. A transition has occurred to a phase where the hexagonal modulations on neighboring PEP sublayers have developed into channels. This is supported by the Fourier modeling to be discussed in the next section. Additional evidence comes from the rheological measurements (Figure 2), which show a sharp increase in G' at the transition at 136 °C from the hexagonally modulated lamellar phase to the hexagonal channel phase. A sequence of SANS experiments as a function of temperature would be required to assess a discontinuous change in the intensity of the four off-meridional peaks at the hexagonal modulated lamellae–hexagonal layered channel phase transition. This will be the subject of future studies on this PEP–PEE polymer. The observation of a hexagonal perforated layer phase is not unique to this sample—it has been observed in a series of other polyolefin diblocks near $f = 0.65$, with different temperature windows of stability.[4] It is important to stress that the SANS results in the third ordered phase were obtained without application of shear; upon 100% strain

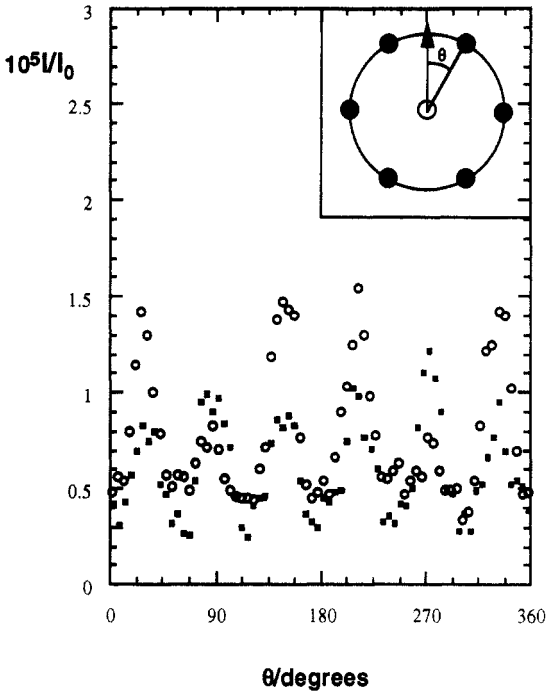

Figure 5. Angular scans for the hexagonally modulated lamellae in the parallel orientation under shear (circles) and after switching off the shear field (squares). The q band was centered on q^*, from $q = 0.013$ to 0.015 Å^{-1}. The measured counts at the detector were divided by the monitor counts to give I/I_0. Inset: definition of the angle θ.

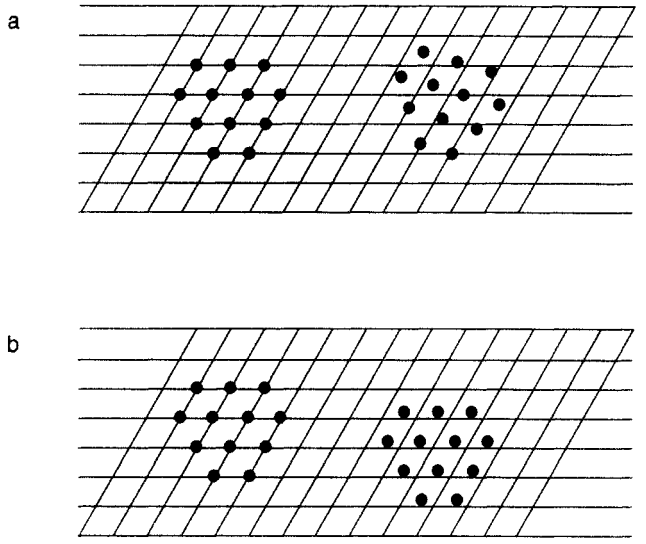

Figure 6. Illustrating the concept of bond orientation order. (a) A liquid has neither long range translational nor bond orientational order. (b) A hexatic phase has long range bond orientational order but no long range translational order. (After Leadbetter.[13])

shearing the pattern in both planes transforms into those found for the highest temperature ordered phase. Therefore we cannot make a firm statement about the thermodynamic stability of this phase. However, evidence for a stable phase comes from the shear modulus behavior on cooling shown in Figure 2b, where a transition from the high temperature (cylinder) phase to the next lowest temperature phase (with $G' \sim 3 \times 10^3$Pa near 140 °C, as on heating) occurs at a lower temperature than on heating; i.e. there is hysteresis associated with this phase transition. A fuller discussion of the relationships between shearing, temperature and phase behavior is deferred to a future paper.[4]

The SANS data at 164 °C indicate a hexagonally packed cylinder structure for the highest temperature ordered

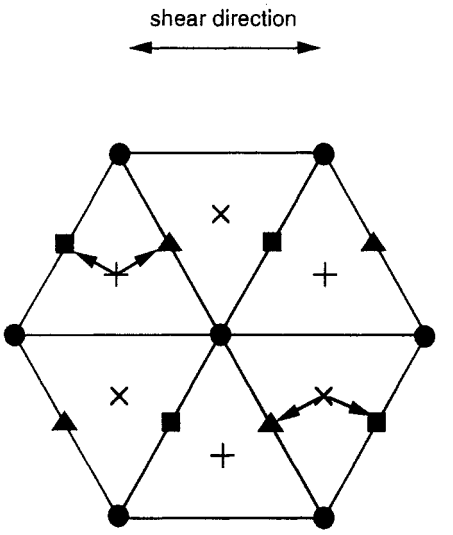

Figure 7. Model for the restacking transition observed for the hexagonally modulated lamellar phase under shear. Positions of modulation maxima in an A layer are shown as circles. In the B layers with no shear field, the B layers may locally be at either of the degenerate close packed positions shown as crosses. Under shear the maxima in B layers are locally at the degenerate positions shown as triangles or squares which are halfway between the layers of circles parallel to the shear direction. This destroys the first order reflections along z, as shown in Figure 4a.

phase. Thus the scattering pattern in the xy plane after large strain shearing and heating from the hexagonal hole phase shows two strong spots, indicating planes of PEE cylinders. The arcing around the spots is presumably the result of orientational disorder of the rods. After shearing, the scattering pattern in the xz plane shows two weak spots, arising from the fact that there is some weak residual layering in the xy plane. A mechanism for the generation of the aligned cylinder phase is illustrated in Figure 8. On heating from the channel phase in the absence of shear, the rods form in the minority component in the three hexagonal directions, giving the scattering pattern in the xy plane shown. The two meridional reflections are about 4 times more intense than the other four, which is consistent with the degeneracy under rotation of these structures. In contrast, the scattering pattern in the xz plane is isotropic, which is consistent with rotational freedom about the y axis for the rod growth. The difference in rod growth in the two orthogonal sample orientations is clearly illustrated by this example (again this anisotropy is also revealed in viscoelastic experiments). The scattering data also reveal that the two length scales evident in the modulated lamellar and channel phases have now collapsed onto a single q^*. Finally, application of a 100% strain, low frequency shear field aligns the rods along the direction of shear, giving the scattering patterns shown in Figure 3d.

Further evidence for a cylinder phase is provided by a PEP–PEE polymer containing 68% PEP ($M_w = 9.3 \times 10^4$) which shows a hexagonal cylinder phase from 95 °C to the ODT at 160 °C.[4] This sample could be cut up in the oriented cylinder phase, unlike the $f = 0.65$ sample in which the cylinder phase does not survive cooling. For the cut-up $f = 0.68$ sample we obtained scattering patterns in three planes; the pattern in the yz plane not observed in the *in situ* sheared samples was hexagonal, confirming a hexagonal rod phase.

5. Fourier Synthesis Models

To model the composition profiles consistent with the scattering patterns for the two intermediate hexagonal

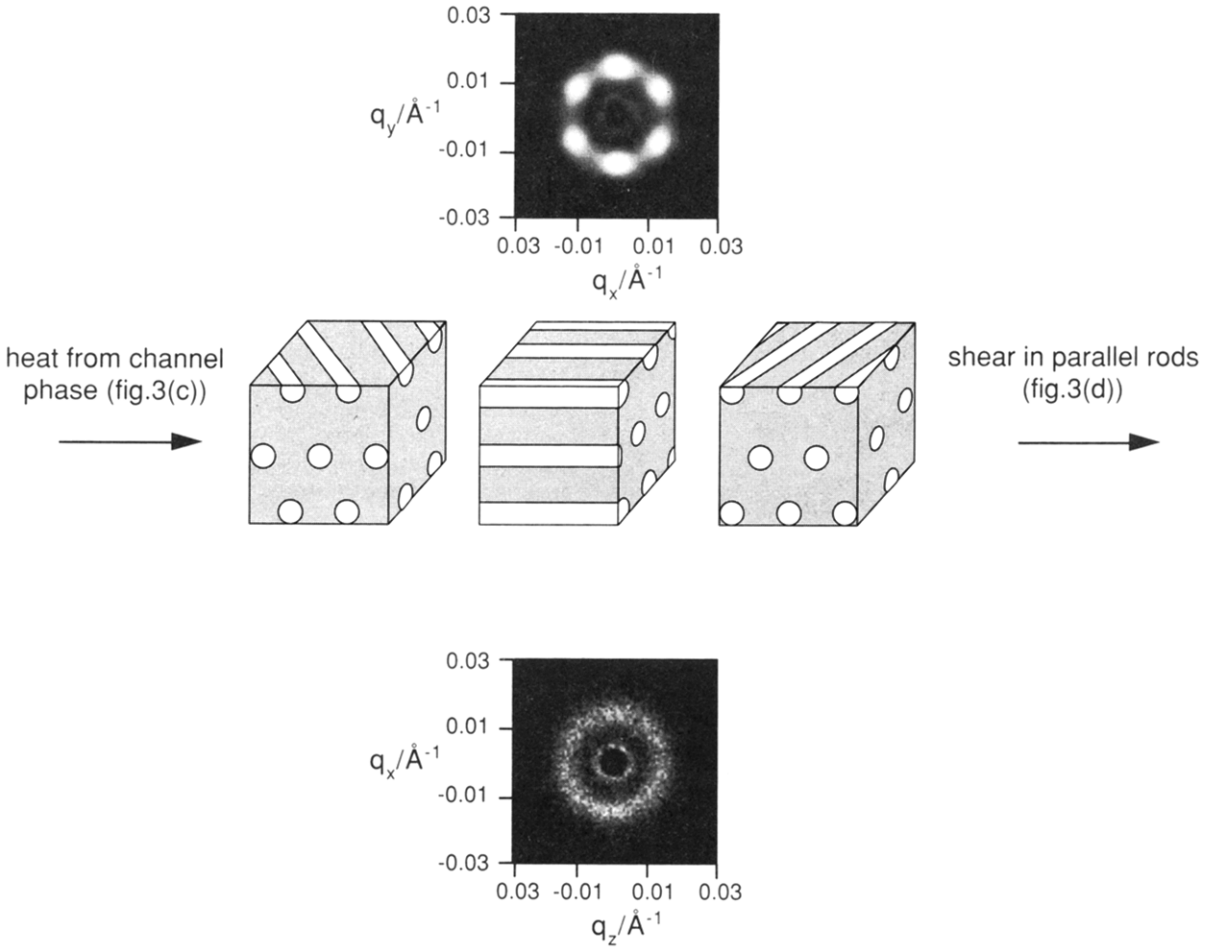

Figure 8. Mechanism for the formation of the rod phase from the channel phase. On heating without shear, rods of the minority component are formed in three degenerate directions corresponding to the in-plane hexagonal axes. The scattering patterns in the perpendicular (top log scale) and parallel (bottom, linear scale) directions consistent with the structural model are also shown. Upon shearing (100% strain, typically $|\dot{\gamma}| = 0.03\ s^{-1}$) the rods align along the shear axis, giving the scattering pattern shown in Figure 3d. The axis system is the same as in Figure 3.

phases, we turned to a Fourier synthesis technique. This does not give additional information not already contained in the SANS patterns but does illustrate graphically the symmetry and topology of the hexagonal mesophases. The density distribution is modeled by assuming that the scattering pattern consists of a number of sharp peaks; i.e. we neglect any influence of the smearing of the reflections. Due to the absence of higher order reflections, it also inevitably yields low resolution images. This approach is consistent with the approach of Leibler, in which the composition profile is expanded as a Fourier series. Thus the density of, say, A blocks is[3]

$$\rho_A(\mathbf{r}) = \sum_k a_k \exp[i(\mathbf{q}_k \cdot \mathbf{r} + \phi_k)] + \text{cc} \qquad (1)$$

Here a_k denotes the amplitude of the kth wave (which for simplificity is taken to be proportional to the intensity of the kth peak peak in the scattering pattern[14]), ϕ_k is a phase factor, and cc denotes complex conjugate.

We have obtained the scattering pattern in only two planes, so a full three-dimensional density map cannot be produced. In the weak scattering direction, a hexagon of reflections of nearly equal intensity is observed, which evidently simply gives a 6-fold density modulation in real space. As mentioned, the scattering pattern is not markedly different in this direction in the modulated lamellar or channel phases.

To assess a topological transformation, the scattering pattern in the xy plane is used to reconstruct density images in the $z = 0$ plane. We will describe in detail a model which is consistent with the SANS data. In this model, the peak positions and intensities observed are used directly to reconstruct a Fourier image, in which the long range order of the modulated layers is destroyed due to the incommensurate wavevectors used in the synthesis. The concept of incommensurability is illustrated by the wavevector diagrams in Figure 9, which also shows how the frustration which is the result of wavevector mismatch can be relieved by formation of closed circuits in two or three dimensions.[18] Due to the absence of three-dimensional periodicity, this is termed an aperiodic model. An alternative model is briefly mentioned, in which a periodic

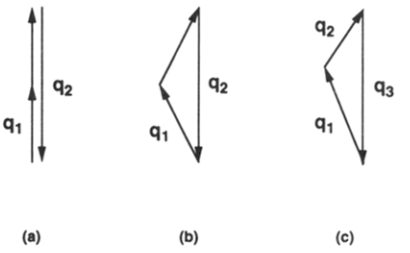

Figure 9. Illustration of incommensurability. (a) Commensurate wavevectors $\mathbf{q}_1$ and the first harmonic $\mathbf{q}_2$ from a closed circuit in one dimension. (b) Two wavevectors are incommensurate but form a closed circuit in two dimensions. This is the case of incommensurate smectic A phases in thermotropic liquid crystals. (c) $\mathbf{q}_1$ and $\mathbf{q}_2$ are again incommensurate, but cannot form a closed circuit in two dimensions. This is the case for the scattering patterns for the intermediate mesophases discussed here.

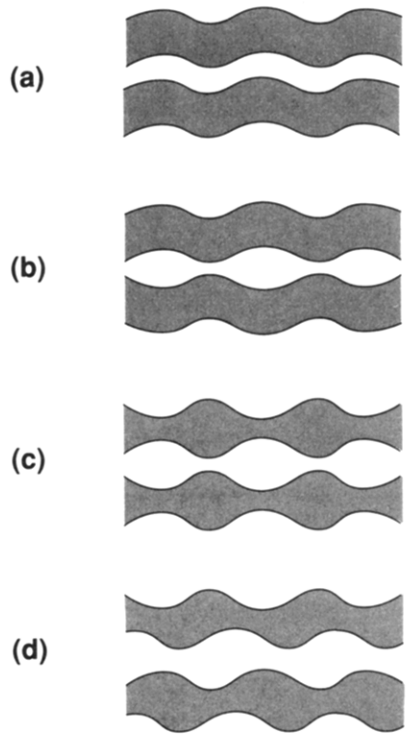

Figure 10. Possible modes of deformation of lamellae illustrated by sections (in the xy plane) through the full three-dimensional structure. (a) Both components are modulated in-phase (undulation mode in two dimensions[13]). (b) The minority component is modulated with a thickness variation, whereas the majority component is modulated with uniform thickness (two-dimensional baroclinic mode). (c) Both components are modulated with thickness variations (2-D peristaltic mode). (d) Both components are modulated with thickness variations, and the total thickness of the layer also varies (2-D second sound mode).

structure is reconstructed. This necessitates the assumption of a twinned structure and the presence of unobserved higher order reflections. This is termed the periodic model.

The available data are used without further assumptions about the scattering pattern in the aperiodic model. To simplify the discussion, centrosymmetric structures are assumed, which reduces the number of possible consistent models considerably, since the phase factor takes on only values of 0 and π. This is consistent with the fact that phase factors within a harmonic in the Leibler mean-field approach are all equal.[7] It may be noted that, by assuming a centrosymmetric structure, we cannot obtain a pure undulation-type deformation for the modulated lamellar phase (Figure 10a). However, baroclinic (Figure 10b) and peristaltic (Figure 10c) type deformations are possible. We use these terms in analogy with the one-dimensional hydrodynamic modes of deformation of lamellae in lyotropic liquid crystals,[17] although in the modulated phase described here the modulation is two-dimensional. There appears to be no mechanism for the stabilization of an undulation mode, as opposed to a baroclinic or peristaltic mode, with a modulation period close to that of the layer periodicity because the line tension only vanishes in the infinite wavelength limit (note that for liquid crystals long wavelength modes are thermally stabilized). Nor do we find a fourth possible deformation, a second sound-type mode (see Figure 10d). This is presumably because it involves asymmetric variations in the modulation maxima and the total layer thickness also varies: in block copolymers there is a strong driving force to minimize variations in domain spacings. We therefore eliminate these as possible modes of deformation.

The image obtained was not affected by the combinations of ϕ_k we chose from 0, π: the models shown here have $\phi_k = 0$. Furthermore, higher order reflections in the modulated lamellar phase (they are missing for the channel phase), with $q_x = 0$, were found to have an intensity $<^1/_{100}$th that of the first order meridional reflections and had a negligible influence on the density maps obtained. They were therefore neglected. With this assumption

$$\rho_A(x,y) = a_1\left[\cos(q_{x,1}x + q_{y,1}y) + \frac{a_2}{a_1}\cos(q_{x,2}x + q_{y,2}y) + \frac{a_2}{a_1}\cos(q_{x,3}x + q_{y,3}y)\right] \quad (2)$$

To illustrate the qualitative differences in the scattering paterns of modulated lamellar and hexagonal channel phases, the data are plotted in Figure 11 as angular scans in a narrow q band centered on q', where q' is the distance of the first order peaks from the origin. At 130 °C, for the parallel orientation $q' = q^* = (0.0144 \pm 0.0002)$ Å^{-1}, whereas in the perpendicular orientation $q' = 1.1q^* = (0.0157 \pm 0.0001)$ Å^{-1}. At 146 °C $q' = q^* = (0.0145 \pm 0.0002)$ Å^{-1} in the parallel orientation and in the perpendicular orientation $q' = 1.1q^* = (0.0160 \pm 0.0002)$ Å^{-1}; this follows the trend for domain spacings to decrease with increasing temperature, this decrease being most rapid in the lamellar phase. At 130 °C the side peaks in the perpendicular orientation (circles) at 48 ± 4° are weak compared to the principal peaks, and comparable in magnitude to the six peaks in the parallel orientation (squares). However, at 146 °C the side peaks at 52 ± 4° have increased substantially compared to the main peaks, which are reduced in height compared to the lower temperature. The six peaks observed in the parallel orientation have not increased significantly in height compared to 130 °C.

Amplitude ratios for the Fourier synthesis were extracted by measuring peak heights in the perpendicular orientation. The peak heights were measured directly from the maxima of the peaks in the angular scans shown in Figure 11. These values were identical to those obtained via a different procedure, fitting the peaks in sector scans (i.e. thin sections through the scattering data at angles where peak maxima are located) to Gaussian functions, and extracting the resulting peak heights. In units of $q' = 1.1q^*$, the scattering vector components are $q_{x,1} = 0$, $q_{y,1} = q'$, $q_{x,2} = q' \sin\theta$, $q_{y,2} = q' \cos\theta$, $q_{x,3} = -q' \sin\theta$, $q_{y,3} = q' \cos\theta$ where $\theta = 50 \pm 4°$. The amplitude ratio used for the modulated phase at 130 °C is $a_2/a_1 = 0.06$, and for the channel phase at 146 °C, $a_2/a_1 = 0.39$. Substituting these parameters into eq 2, the Fourier reconstructed density plots shown in Figure 12 are obtained. As noted previously, the waves in the reconstruction of eq 2 are not commensurate and we have chosen to represent the density only in the interval from $-2d$ to $2d$, where d is the domain spacing, $2\pi/(1.1q^*)$.

The image in Figure 12a is consistent with a modulated lamellar structure, both components being continuous. The modulation has a small amplitude, evident from the weakness of the side peaks in the scattering pattern. No single mode of deformation is present in these images—in the region shown, both baroclinic and peristaltic type modulations are evident. Figure 12b is reconstructed from the same set of wavevectors, but with higher amplitudes for the side peaks: at the higher temperature, channels have formed; however it is not clear whether the structure is mono- or bicontinuous. This could only be confirmed by reconstruction of a full three-dimensional density image. However, we favor a monocontinuous structure because

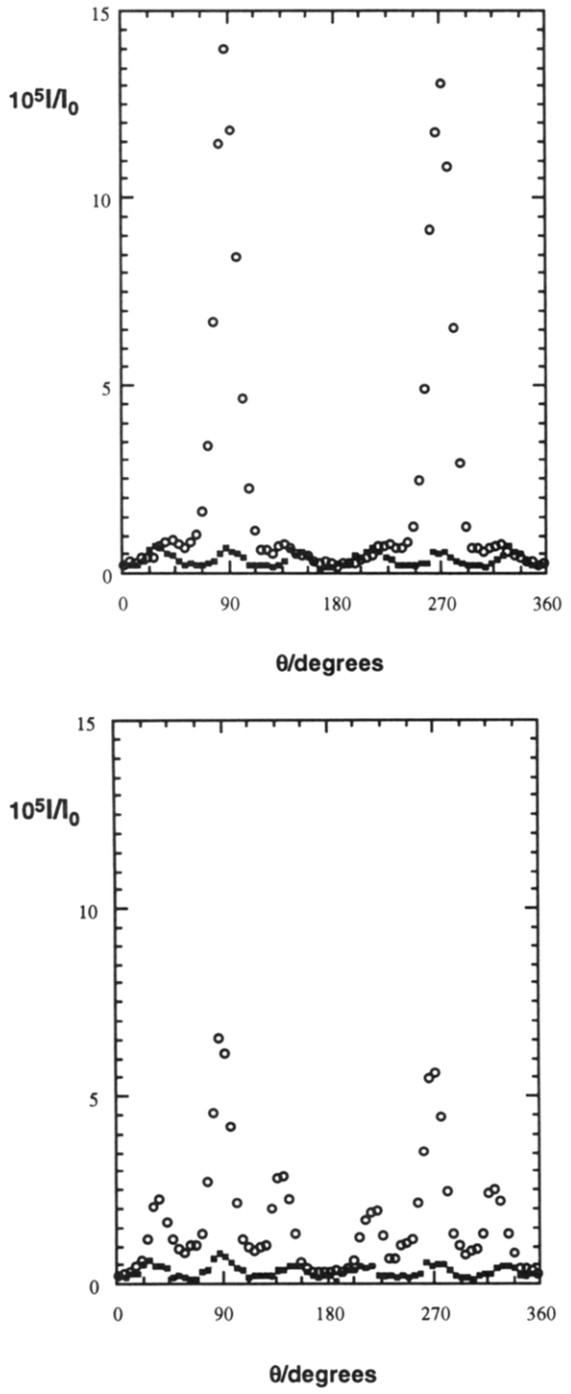

Figure 11. Angular scans for parallel (■) and perpendicular orientations (○): (a, top) 130 °C; (b, bottom) 146 °C. For the former the q band was q = (0.013–0.015) Å^{-1}, whereas for the latter it was q = (0.014–0.016) Å^{-1}. The angle θ is defined with respect to the vertical in the scattering patterns in Figure 4.

this would form naturally from the baroclinic mode deformation of modulated lamellae (see Figure 3).

Large strain shear causes the side peaks in the scattering patterns in the modulated lamellar phase to move to 56 ± 2° (Figure 4b), i.e. nearer the two-dimensional wavevector matching condition at 60° (see Figure 9). This means that, under shear, within this model the translational order becomes more long range. For the channel phase, large strain shearing leads to scattering patterns resembling those for cylinders, which leads us to believe that this phase transforms to rods under appropriate shearing conditions (we have yet to study fully the effect of different shearing conditions on either of these phases).

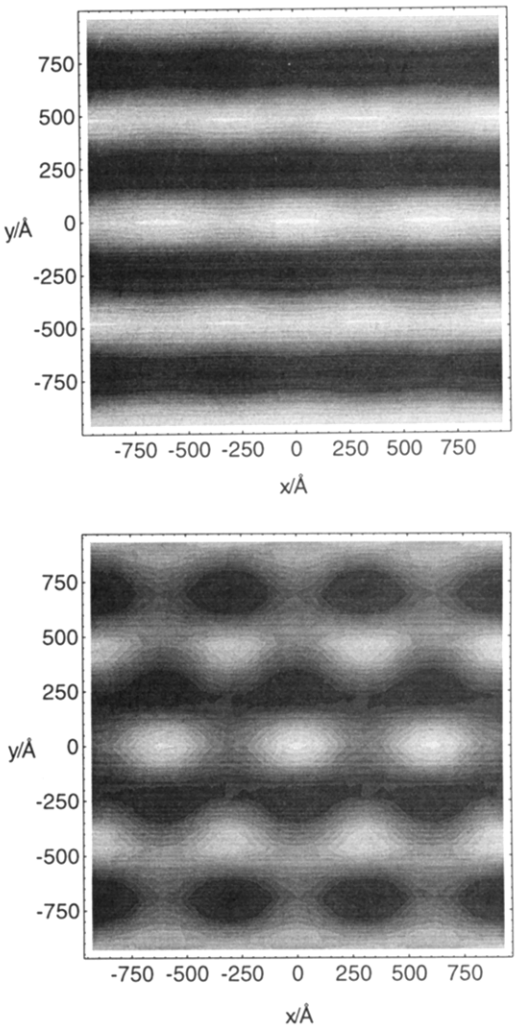

Figure 12. Fourier images reconstructed using the Fourier series (2) for the aperiodic model. The density in the xy plane is represented by 15 equally spaced levels. Similar structures are observed outside this area. (a, Top) At 130 °C modulated lamellae can be seen. (b, Bottom) At 146 °C, channels have clearly formed.

An alternative to the aperiodic model presented here might be a model with solely baroclinic- or peristaltic-type deformations, with short range translational order but long range bond orientational order. This however is much less straightforward to model than the Fourier technique discussed here, and a full treatment of the scattering from fluctuating lamellae will be presented elsewhere.

Periodicity could be restored in the xy plane by hypothesizing a twinned structure (see Figure 13) with a scattering pattern containing one of the pair of four side peaks (at ±50° with respect to the meridian). Then two additional peaks would result from the periodicity at ±65° to the meridian at 1.86q* (see Figure 14). These are not observed, and we do not favor this model for this reason. In addition, Fourier reconstructions within a periodic model (not shown) show that the modulations are not symmetric about a vertical line. In addition, the layer thickness is seen to vary in this case: this is highly unfavorable for block copolymers, which have the conformational flexibility to maintain a uniform domain spacing.[19]

6. Discussion

In summary, we have used dynamic elastic shear modulus and SANS experiments to study the phase

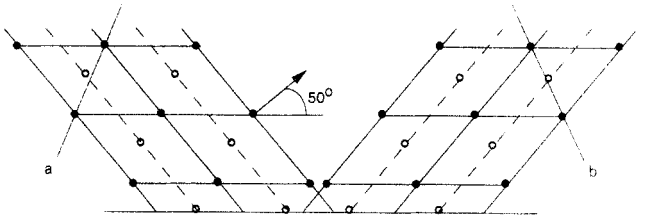

Figure 13. Twinned monoclinic structure (xy plane) proposed as a commensurate model. The filled circles indicate modulation maxima for the majority component in the plane of the paper; the open circles represent these maxima in neighboring layers above and below the plane of the page. The presence of commensurate periodicities in two directions necessarily introduces a third periodicity in a different direction. The planes corresponding to the maxima of these waves are shown as a and b for the two twinned structures.

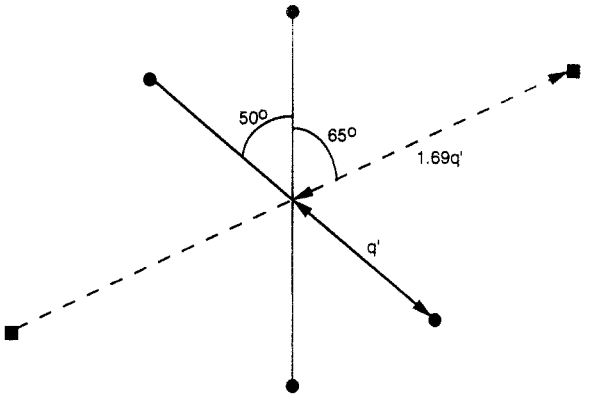

Figure 14. Scattering pattern expected from the principal planes of the monoclinic twinned structure shown on the right hand side of Figure 13.

behavior of an asymmetric diblock copolymer near the order–disorder transition. Two phases intermediate between classical lamellar and hexagonal cylinder phases were observed on varying the temperature. Similar results have been obtained with several other polyolefin diblock copolymers, indicating that these phases are ubiquitous near $f = 0.65$. On the basis of SANS patterns obtained on samples that had previously been subjected to oscillatory shear we identify the low temperature intermediate phase as hexagonally modulated lamellae, while the high temperature one consists of layered hexagonally packed channels.

A Fourier modeling method has been introduced as a simple technique for visualizing the structures of these phases using the peak positions and intensities in the scattering patterns. In an aperiodic model the SANS patterns are taken at face value and the incommensurability in the perpendicular orientation leads to the destruction of long range translational order between layers. On the other hand, the 6-fold symmetry of the scattering patterns in the parallel orientation implies the existence of in-plane bond orientational order. For the modulated lamellar phase, this is reminiscent of the defining properties of the hexatic B phase found in some thermotropic liquid crystals.[20] The extent of intra- versus interplane order cannot be established from our experiments due to the broad resolution function in the neutron scattering experiments. A proof of a hexatic phase from scattering studies would require a detailed line shape analysis, as done for the high resolution X-ray diffraction studies of thermotropic liquid crystals.[21] In a periodic model we obtain a monoclinic structure, which is difficult to accept physically due to the asymmetric deformations of lamellae or channels and variations in the domain spacing which result. In addition, we have considered the effect of shear on the modulated lamellar phase and discussed a possible restacking transition under shear. The channel phase transforms into rods when subjected to large amplitude shear.

In the aperiodic model for the modulated lamellar phase, long range translational order is destroyed due to fluctuations in the positions of layers. This is the well-known Landau–Peierls effect, which has been confirmed experimentally for thermotropic smectic A phases.[21] It thus appears that this intermediate phase is a consequence of compositional fluctuations. These fluctuations are evidently anisotropic, unlike fluctuations in the disordered melt. Anisotropic fluctuations have not been treated theoretically, indeed, in a recent self-consistent treatment of fluctuations in lamellar block copolymers Barrat and Fredrickson[22] excluded the possibility of anisotropic fluctuations by making the approximation of an isotropic form for the structure factor in the lamellar phase.

The important role of composition fluctuations in modifying block copolymer phase behavior near the ordering transition was first noted by Leibler and studied in detail (using the structure factor for the disordered state) by Fredrickson and Helfand.[23] The essential result for our purposes is that the phase diagram becomes less mean-field like as the degree of polymerization is lowered, and the mean-field result is recovered in the limit $N \rightarrow \infty$.

Recent experiments have confirmed this aspect of fluctuation theory predictions, both in the disordered melt[24] and in the lamellar phase.[25] We believe that our present results showing nonclassical phases near the order–disorder transition can be rationalized in terms of the effects of finite molecular weight. Fluctuation effects can stabilize nonclassical phases, as demonstrated recently by Brazovskii and co-workers.[26] They showed that fcc and simple cubic phases can become absolutely stable when fluctuations are accounted for in a Landau-type theory, however the structures discussed here have not yet been considered within fluctuation theory.

In support of the picture of classical phase behavior in the strong segregation limit, Fredrickson has recently considered the formation of nonclassical structures, for example bicontinuous phases, in strongly segregated block copolymers.[27] He allowed for the nonuniform stretching of the chains in the Wigner–Seitz cell for the hexagonal rod phase as an example of a system with a nonspherical Wigner–Seitz cell. He confirmed earlier calculations, in which nonuniform chain stretching was not allowed for, indicating that ordered bicontinuous double diamond and "catenoid lamellar" (channel) phases are not stable in the strong segregation limit ($\chi N \rightarrow \infty$).

A hexagonal catenoid lamellar structure (i.e. hexagonal perforated layer phase) was predicted theoretically by Olvera de la Cruz *et al.*[7] They added harmonic corrections to Leibler's mean-field theory for diblocks, considering only the region of the phase diagram near $f = 0.5$. They found that a hexagonal ABAB structure was more stable than lamellae near the ODT. However, it has subsequently been shown that harmonic corrections to Leibler's theory cannot account for stable layered hexagonal mesophases near the order–disorder transition.[5] It would be interesting to allow for the hexatic nature of these phases, which do not have long range hexagonal ABAB order.

The Leibler mean-field phase diagram may be modified by an additional parameter related to the flexibilities and space-filling abilities of the two blocks, which are in general different. This has been described in terms of different

statistical segment lengths for the blocks, defined on a unit volume basis which is consistent with unit volume definitions of χ and f.[1,4] The segment length, b, is contained in the definition of the unperturbed mean square radius of gyration, $R_g^2 = b^2N/6$. A conformational asymmetry parameter may account for the observed asymmetry in ordering temperatures on either side of $f = 0.5$ in the diblock phase diagram. It may also account for the asymmetry in the regions of stability of the classical phases and the asymmetry in the types of nonclassical phases on either side of the symmetric case, $f = 0.5$. Thus at $f = 0.39$ there is evidence for bicontinuous phases, while at $f = 0.65$ we observed the two intermediate hexagonal phases described here, at least one of which is not bicontinuous.

An analogous phase to the hexagonal hole phase has been observed for lyotropic liquid crystals between lamellar and hexagonal rod phases.[28-31] The structure of this hexagonal intermediate phase is not firmly established, but it has been considered as a hexagonally perforated lamellar phase.[31] There appears to be no analogue for the modulated hexagonal phase in amphiphilic systems, although rippled lamellar phases have been described.[32] Presumably, a hexagonally modulated lamellar phase is unstable for low molecular weight surfactants due to the high cost in curvature energy, while it may exist for block copolymers due to the greater degree of conformational freedom of the block copolymer chains compared to the amphiphilic chains. In fact, preliminary experiments with a higher molecular weight $f = 0.65$ polyolefin system (poly(ethylenepropylene)–poly(ethylene) $M_w = 1.64 \times 10^5$) suggest that the modulated lamellar phase exists over an even greater temperature range. Layered phases with in-plane hexagonal order have also been observed in thermotropic liquid crystals,[21] thin ferrimagnetic layers,[33] weakly supercritical convective systems,[34] and Turing patterns in a gel reactor.[35]

In the hexatic smectic B phase in liquid crystals the layers are decoupled (quasi long range translational order normal to the layer, short range order within a layer[21]), while bond orientational order is long range. One apparent problem concerning our analogy between the hexagonally modulated lamellar phase and the hexatic B phase is that this phase appears on heating the lamellar phase, which is analogous to the smectic A phase in liquid crystals. In liquid crystals, heating causes the layers of the hexatic B phase to melt and the lamellar phase is the high temperature phase. However, unlike thermotropic liquid crystals, heating a lamellar diblock copolymer will lead to a hexagonal cylindrical phase, as shown here. In other words, the phase symmetry increases to that of a two-dimensional hexagonal crystal on heating, whereas a three-dimensional hexagonal crystal phase occurs below the hexatic phase in liquid crystals. The Fourier synthesis does not give a unique picture of the deformations of the lamellae. An alternative to the resulting mixed mode structure in the incommensurate model would have short range translational order of lamellae with the same mode of deformation, which we believe is baroclinic on the basis of stacking considerations that we have discussed.

Both the translational and bond orientational order in crystalline smectic B phases is three-dimensional.[21] Sirota and co-workers have recently observed modulated phases in crystalline B liquid crystals.[36] On the basis of satellite reflections observed near the Bragg peaks, they have identified one-dimensional and two-dimensional square modulated structures. In addition they observed a sequence of layer restacking transitions, which however does not include the monoclinic I structure observed here. The modulated structures observed by them occur in a three-dimensional system and correspond to long wavelength modes which they have attributed to the formation of defect-separated domains. This is different from the deformations which we have described in the one-dimensional lamellar phase, which are not associated with defects.

Analogies also exist with two-dimensional magnetic thin films where stripe and bubble phases occur, which are two-dimensional lamellar and hexagonal phases.[33,37] The deformations of the stripe phase when subjected to a dilative strain at zero magnetic field which eventually results in a labyrinthine disordered phase have recently been studied by Seul and Wolfe.[38] They show that the temperature-induced reduction of the layer spacing results in an undulation mode deformation of the stripes. This appears to be the same driving force for the formation of the modulated lamellar phase we have observed (although the deformation mode is not the same). The amplitude of the modulations increases continuously until eventually a threshold is reached, where a chevron structure with a discontinuity between domains becomes stable. Finally, via mechanisms of disclination formation and subsequent unbinding, a labyrinthine phase is formed, where there is no long range order. From this and from our discussion of liquid crystal phases, it seems that there are fascinating analogies between block copolymers and other mesomorphic systems which result from their common origin as symmetry-breaking fluctuating systems.

Acknowledgment. Support for this research was provided by the U.S. Air Force Office of Scientific Research (AFOSR-90-0207) and the Center for Interfacial Engineering, a National Science Foundation Engineering Research Center at the University of Minnesota. We acknowledge the support of NIST, U.S. Department of Commerce, in providing some of the facilities used in this work, and NATO for a travel grant.

References and Notes

(1) Almdal, K.; Koppi, K. A.; Bates, F. S.; Mortensen, K. *Macromolecules* **1992**, *25*, 1743.
(2) Förster, S.; Khandpur, A. K.; Bates, F. S. To be published.
(3) Leibler, L. *Macromolecules* **1980**, *13*, 1602.
(4) Hamley, I. W.; Koppi, K. A.; Rosedale, J. H.; Schulz, M. F.; Bates, F. S.; Almdal, K.; Mortensen, K. Manuscript in preparation.
(5) Hamley, I. W.; Bates, F. S. To be published.
(6) Marques, C. M.; Cates, M. E. *Europhys. Lett.* **1990**, *13*, 267.
(7) Olvera de la Cruz, M.; Mayes, A. M.; Swift, B. W. *Macromolecules* **1992**, *25*, 944.
(8) Bates, F. S.; Rosedale, J. H.; Bair, H. E.; Russell, T. P. *Macromolecules* **1989**, *22*, 2557.
(9) Koppi, K. A.; Tirrell, M.; Bates, F. S.; Almdal, K.; Colby, R. H. *J. Phys. II* **1992**, *2*, 1941.
(10) Hadziioannou, G.; Mathis, A.; Skoulios, A. *Colloid Polym. Sci.* **1979**, *257*, 136.
(11) The results in Figure 2 are for a sample with lamellae in the parallel orientation (see Figure 1). This has been determined by mounting samples presheared on a parallel plate device similar to that used for the SANS experiments in different orientations in the rheometer. The sample orientation in a previous study[1] was not determined in this way. Furthermore, the heating rate was more rapid than that used here. Experiments where the heating rate has been varied confirm that the drmatic increase in G' in the third ordered phase is kinetically controlled.
(12) For example, the fully hydrogenous version of this material appears to exhibit only three ordered phases, as evidenced by the absence of the sharp peak in G' at about 150 °C (see Figure 2). Furthermore, T_{ODT} increases by about 18 °C when hydrogen

is used instead of deuterium in the saturation reaction. We will expand on these comments in ref 4.

(13) Leadbetter, A. J. In *Thermotropic Liquid Crystals*; Gray, G. W., Ed.; Wiley: Chichester, U.K., 1987.
(14) We have used an intensity ratio rather than a square-root intensity ratio to mimic the effect of anisotropic damping of the density waves, $\cos[\mathbf{q}_k \cdot \mathbf{r} + u(\mathbf{r})]$, where $u(\mathbf{r})$ denotes a layer fluctuation amplitude. The inclusion of the phase factor $u(\mathbf{r})$ is consistent with the order parameter for a layer phase.[15] For a hexatic phase, a model allowing properly for the anisotropic fluctuations might be constructed along the lines of that for hexatic membranes.[16] This is however beyond the scope of this paper.
(15) De Gennes, P. G. *The Physics of Liquid Crystals*; Clarendon Press: Oxford, U.K., 1975.
(16) Nelson, D. R.; Peliti, L. *J. Phys.* (*Paris*) **1987**, *48*, 1085.
(17) Nallet, F.; Roux, D.; Prost, J. *J. Phys.* (*Paris*) **1989**, *50*, 3147.
(18) Prost, J. *Adv. Phys.* **1984**, *33*, 1.
(19) Helfand, E.; Wasserman, Z. R. In *Developments in Block Copolymers*; Goodman, I., Ed.; Applied Science: New York, 1982; Vol. 1.
(20) Pindak, R.; Moncton, D. E.; Davey, S. C.; Goodby, J. W. *Phys. Rev. Lett.* **1981**, *46*, 1135.
(21) Pershan, P. S. *Structure of Liquid Crystal Phases*; World Scientific: Singapore, 1988.
(22) Barrat, J.-L.; Fredrickson, G. H. *J. Chem. Phys.* **1991**, *95*, 1281.
(23) Fredrickson, G. H.; Helfand, E. *J. Chem. Phys.* **1987**, *87*, 697.
(24) Bates, F. S.; Rosedale, J. H.; Fredrickson, G. H.; Glinka, C. J. *Phys. Rev. Lett.* **1988**, *61*, 2229.
(25) Rosedale, J. H.; Bates, F. S.; Almdal, K.; Mortensen, K. Manuscript in preparation.
(26) Brazovskii, S. A.; Dzyaloshinskii, I. E.; Muratov, A. R. *Sov. Phys. JETP* **1987**, *66*, 625.
(27) Fredrickson, G. H. Preprint.
(28) Luzzati, V.; Tardieu, A.; Gulik-Krzywicki, T. *Nature* **1968**, *217*, 1028.
(29) Luzzati, V.; Gulik-Krzywicki, T.; Tardieu, A. *Nature* **1968**, *218*, 1031.
(30) Kekicheff, P.; Cabane, B. *Acta Crystallogr., Sect. B* **1988**, *44*, 395.
(31) Kekicheff, P.; Tiddy, G. J. T. *J. Phys. Chem.* **1989**, *93*, 2520.
(32) Leibler, S.; Andelman, D. *J. Phys.* (*Paris*) **1987**, *48*, 2013.
(33) Seul, M.; Monar, L. R.; O'Gorman, L.; Wolfe, R. *Science* **1991**, *254*, 1616.
(34) Malomed, B. A.; Tribel'skii, M. I. *Sov. Phys. JETP* **1987**, *65*, 305.
(35) Ouyang, Q.; Swinney, H. L. *Nature* **1991**, *352*, 610.
(36) Sirota, E. B.; Pershan, P. S.; Deutsch, M. *Phys. Rev. A* **1987**, *36*, 2902.
(37) Garel, T.; Doniach, S. *Phys. Rev. B* **1982**, *26*, 325.
(38) Seul, M.; Wolfe, R. *Phys. Rev. A* **1992**, *46*, 7519, 7534.